Ductiletobrittle transition in fibrereinforced concrete beams: Scale and fibre volume fraction effects

Received: 26 November 2019 | Revised: 6 December 2019 | Accepted: 9 December 2019

DOI: 10.1002/mdp2.127

SPECIAL ISSUE ARTICLE

WILEY

Ductile-to-brittle transition in fibre-reinforced concrete beams: Scale and fibre volume fraction effects

Federico Accornero | **Alessio Rubino** | **Alberto Carpinteri**

Department of Structural, Geotechnical and Building Engineering, Politecnico di Torino, Torino, Italy

Correspondence
Federico Accornero, Department of Structural, Geotechnical and Building Engineering, Politecnico di Torino, 24 C.so Duca degli Abruzzi, 10129 Torino, Italy.
Email: federico.accornero@polito.it

Abstract

The mechanical response of fibre-reinforced brittle-matrix structural elements subjected to bending is discussed in the framework of fracture mechanics. By means of numerical simulations based on the bridged crack model, the flexural behaviour of steel fibre-reinforced concrete (FRC) beams has been investigated, taking into account pull-out or yielding bridging mechanism of the secondary phase. In both cases, the numerical results predict a transition of the global structural behaviour, which can range from ductile to catastrophic. This behaviour is governed by a dimensionless parameter, the brittleness number, N_P, in which the effects of the structural size and the fibre volume fraction are included. An experimental campaign is carried out on FRC beams subjected to three-point bending tests, considering three different beam sizes and four different fibre contents. A comparison between experimental tests and numerical simulations shows that the bridging mechanism is due to the fibre slippage into the matrix, rather than the fibre plastic flow. The expected ductile-to-brittle transition is found for each beam scale, as predicted by N_P. As a consequence, the minimum fibre volume fraction can be defined according to this model, providing an effective structural bearing capacity of FRC structural members.

KEYWORDS

bridged crack model, constitutive laws, ductile-to-brittle transition, fibre-reinforced composites, fibre volume fraction effect, minimum reinforcement, scale effect fibre

1 | INTRODUCTION

In recent years, a significant part of structural engineering makes a wide use of fibre-reinforced concrete (FRC), ie, a cementitious brittle matrix (mortar, concrete) coupled with a secondary phase represented by reinforcing fibres, randomly orientated and distributed within the volume of the composite. For this material, the secondary phase plays a key role related to the bridging action, which affects both the macrocracks and the microcracks in the process zone, so as to prevent their coalescence, opening, and growth. These bridging toughening mechanisms are due to debonding, sliding, and frictional pulling-out between the matrix and the high-resistance fibres or to yielding of the low-resistance ductile fibres. They result in an improved global structural response of the component, due to an increase of several mechanical properties: flexural and compressive strengths, fracture toughness, and ductility.[1] In this context, knowledge of the mechanical behaviour of these materials leads to an improvement in the material design through an optimization of the components. The bridged crack model[2–4] is a fracture mechanic-based approach able to describe the mechanical response of fibre-reinforced beams in bending, taking into account the brittle-matrix behaviour, and the reinforcement action, that can be represented either by yielding or slippage. During the last decades, different versions of this model have been used to describe the crack propagation process in materials with diffused reinforcements in the matrix and materials reinforced with a small number of elements.[5–7] The model has been validated both for monotonically increasing or cyclic loading.[8–10] In all cases, the bridged crack model

reproduces and explains the constitutive flexural response of concrete composites, which is characterized by discontinuous phenomena in the postcracking phase, ie, snap-back and snap-through instabilities. It is worth noting that snap-back and snap-through branches can be captured under deflection or load control, respectively. The model is able to predict a transition in the global structural response, which can range from ductile to catastrophic. This ductile-to-brittle transition can be described by a dimensionless parameter called brittleness number, N_P. This parameter is a function of the toughness of the matrix, of the yielding or slippage limit of the fibre-reinforcement, of the fibre volume fraction of the reinforcement, and of the characteristic structural size. In this work, the bridged crack model with multiple fibres has been successfully validated on the basis of an experimental campaign carried out at the Fracture Mechanics Laboratory of Politecnico di Torino. Three-point bending (TPB) tests have been carried out on notched FRC beams, characterized by three different sizes (h = 50 mm; 100 mm; 200 mm) and four different fibre volume fractions (V_f = 0.08%, 0.20%, 0.96%, and 1.28%). In this way, it has been possible to study the ductile-to-brittle transition in FRC beams subjected to bending.[11–17] Moreover, a minimum critical value of fibre volume fraction can be evaluated, providing a ductile postpeak response of FRC members, avoiding any loss in the structural bearing capacity.

2 | NUMERICAL SIMULATIONS

As briefly introduced in the previous section, the bridged crack model is able to describe the flexural behaviour of a fibre-reinforced brittle-matrix beam, characterized by a rectangular cross section, an edge crack, and subjected to an applied bending moment M. The geometry of the model is shown in Figure 1, where h and t are the section height and thickness, respectively; a is the initial crack depth; and h_i, i = 1, … n defines the position of the generic fibre reinforcement. A normalized crack depth $\xi = a/h$, and a normalized position of the generic fibre reinforcement $\zeta_i = h_i/h$ can be defined. The fibre reinforcements crossing the crack are considered as active, exerting a bridging action described by the forces F_i (Figure 1).

Within the bridged crack model, the fracture process zone of FRC beams is considered as sufficiently small, since it is confined to the interspace between two subsequent fibre reinforcements. Under these circumstances, the concepts of linear elastic fracture mechanics are fully applicable: the composite matrix is then assumed to be elastic-perfectly brittle and it is characterized by the fracture toughness, K_{IC}, and the Young modulus, E. On the other hand, a rigid-perfectly plastic constitutive law is assumed for the reinforcements (Figure 2), characterized by the ultimate force, F_P, in both the yielding and slippage hypothesis. In the hypothesis of yielding, F_P represents the force that makes the fibre plastically flow (Equation (1)). In the hypothesis of slippage, F_P is related to the frictional bonding force, acting on the lateral surface of the fibre (Equation (2)):

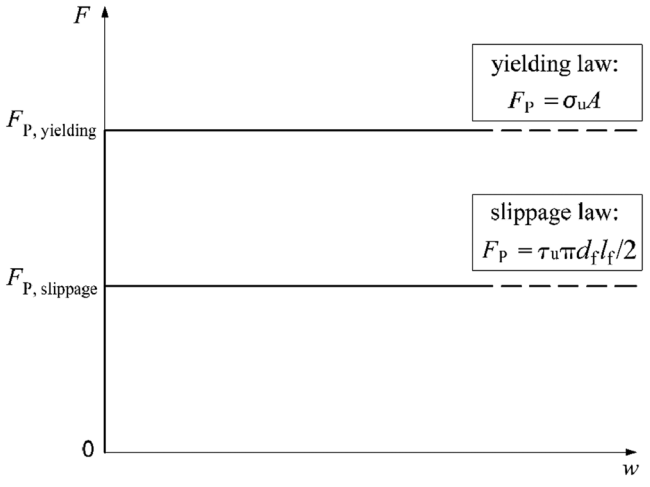

FIGURE 2 Reinforcement constitutive laws: Fibre yielding or slippage

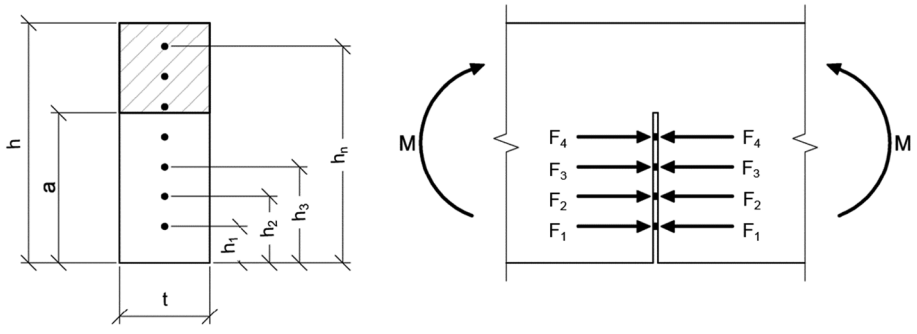

FIGURE 1 Fibre-reinforced brittle-matrix beam model

$$F_{P,i} = \sigma_u A_i, \tag{1}$$

$$F_{P,i} = \tau_u \pi d_{f,i} \frac{l_{f,i}}{2}, \tag{2}$$

where A_i is the fibre cross-sectional area, σ_u and τ_u represent the ultimate stress related to the bridging mechanism of yielding or slippage, whereas d_f and l_f are the diameter and the length of the fibre, respectively.

The mathematical problem consists in the determination of the crack opening displacements and the reinforcement actions, for each reinforcement level. By using the superposition principle, these quantities can be described by the following relationship:

$$\{w\} = \{\lambda_M\} M - [\lambda]\{F\}, \tag{3}$$

where the minus sign is due to the crack-closure action exerted by the active reinforcements. Being the problem statically indeterminate, as the fibre reactions are unknown, the compatibility displacement conditions are introduced for the cracked cross section. Considering a rigid-perfectly plastic behaviour for the fibres, the crack results to be closed until the ultimate force, $F_{P,i}$, is reached. Then, the fibre reactions can be calculated, as a function of the applied bending moment M, and by solving the following linear equation system:

$$[\lambda]\{F\} = \{\lambda_M\} M. \tag{4}$$

When a fibre reaches the ultimate force related to yielding or slippage mechanism, the fibre reaction becomes known and equal to $F_{P,i}$, whereas the crack opening displacement at the same level becomes greater than zero. From this point forward, the problem is solved by partitioning the system of Equation (3). In addition to yielding or slippage crisis of the reinforcement fibres, the model includes also the crack propagation phenomenon occurring within the cross section. The crack propagation condition, defined in agreement with linear elastic fracture mechanics, states that the crack propagates when the stress-intensity factor reaches its critical value, K_{IC}, namely, the fracture toughness of the matrix. Consistently with the theoretical framework of the model, the stress-intensity factor, K_I, is evaluated in virtue of the superposition principle[18,19]:

$$K_I = K_{I,M} - \sum_{i=1}^{n} K_{I,i}, \tag{5}$$

where the sum of two contributions emerges, one due to the external bending moment, the other taking into account the fibres bridging action. Equations (3) to (5) enable to fully describe the mechanical response of fibre-reinforced structural elements in bending in terms of applied bending moment and localized rotation. With particular regards to the postcracking phase, the model is able to capture local discontinuity phenomena, ie, snap-back and snap-through instabilities, represented by virtual branches, as extensively reported in previous studies.[9,20,21] The stability of the fracturing process of the cracked beam section can also be discussed by a global point of view. It is worth noting that the global response, which can range from ductile to catastrophic, is governed by a dimensionless parameter called brittleness number,[3,9] N_P, which is a function of the volume fraction of the reinforcement V_f ($V_f = \rho$, being ρ the fibre fraction in the cross-section area); the fracture toughness of the matrix, K_{IC}; the characteristic structural size, h; and a generalized ultimate stress, σ_u or τ_u, related to the fibre bridging mechanism:

$$N_P = \rho \sqrt{h} \frac{\sigma_u}{K_{IC}}, \tag{6}$$

for the yielding mechanism, and

$$N_P = \rho \sqrt{h} \frac{\tau_u \lambda_f}{K_{IC}}, \tag{7}$$

for the slippage mechanism.

In this latter case, the relationship between the shear stress, τ_u, acting on the lateral surface of the reinforcement, and the corresponding axial stress, σ_u, acting on the cross-sectional area of the fibre, is found as

$$F_P = \sigma_u A = \sigma_u \pi \frac{{d_f}^2}{4} = \tau_u \pi d_f \frac{l_f}{2}, \tag{8}$$

explaining the dependence of the brittleness number on the fibre aspect ratio, $\lambda_f = 2l_f/d_f = l_f/r_f$. As a result, in the slippage hypothesis, the brittleness number still depends on the reinforcement volume fraction, V_f, on the matrix fracture toughness, K_{IC}, and on the ultimate stress describing the bridging mechanism, τ_u, but it is also affected by the geometric parameter describing the fibre. In both cases, the critical value of the brittleness number, N_{PC}, defines the so-called minimum reinforcement condition.[9] The bridged crack model has been used to investigate the flexural behaviour of FRC beams in bending, by varying the structural size, the fibre volume fraction, and considering two different bridging mechanisms (yielding or slippage). In particular, in the present work, three different beam sizes (h = 50 mm, 100 mm, and 200 mm) and eight different fibre volume fractions depending on the fibre bridging mechanism are taken into account. A continuous reinforcement distribution has been modelled, considering a fibre number $n > 20$, since it represents the asymptotical condition for a number of fibres $n \to \infty$.[9] In Figures 3A to 3C, the flexural behaviour of 24 beams subjected to TPB test is described by means of the bridged crack model in terms of load vs midspan deflection, considering a yielding bridging mechanism of the fibres. These diagrams are obtained considering the concrete fracture toughness K_{IC} = 19 MPa$\sqrt{\text{mm}}$, and the concrete Young's modulus E = 31500 MPa. The fibre yielding stress is assumed as σ_u = 1100 MPa.

In Figures 4A to 4C, the design abacus is obtained considering a slippage mechanism between the matrix and the steel fibres. In this case, the ultimate shear stress is evaluated as a function of the mean compressive strength of the concrete matrix.

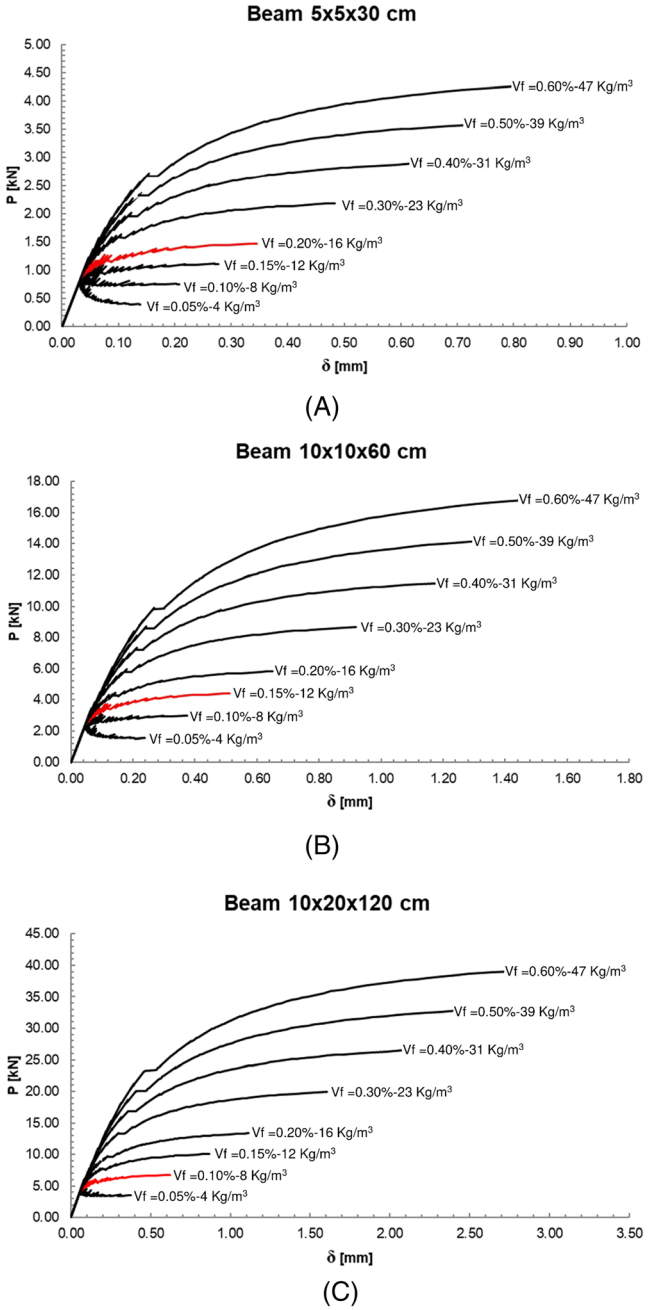

FIGURE 3 Design abacus based on fibre yielding mechanism. The numerical results are described in terms of load vs midspan deflection for beam size h = 50 mm (A); h = 100 mm (B); h = 200 mm (C). The red curve indicates the minimum reinforcement condition

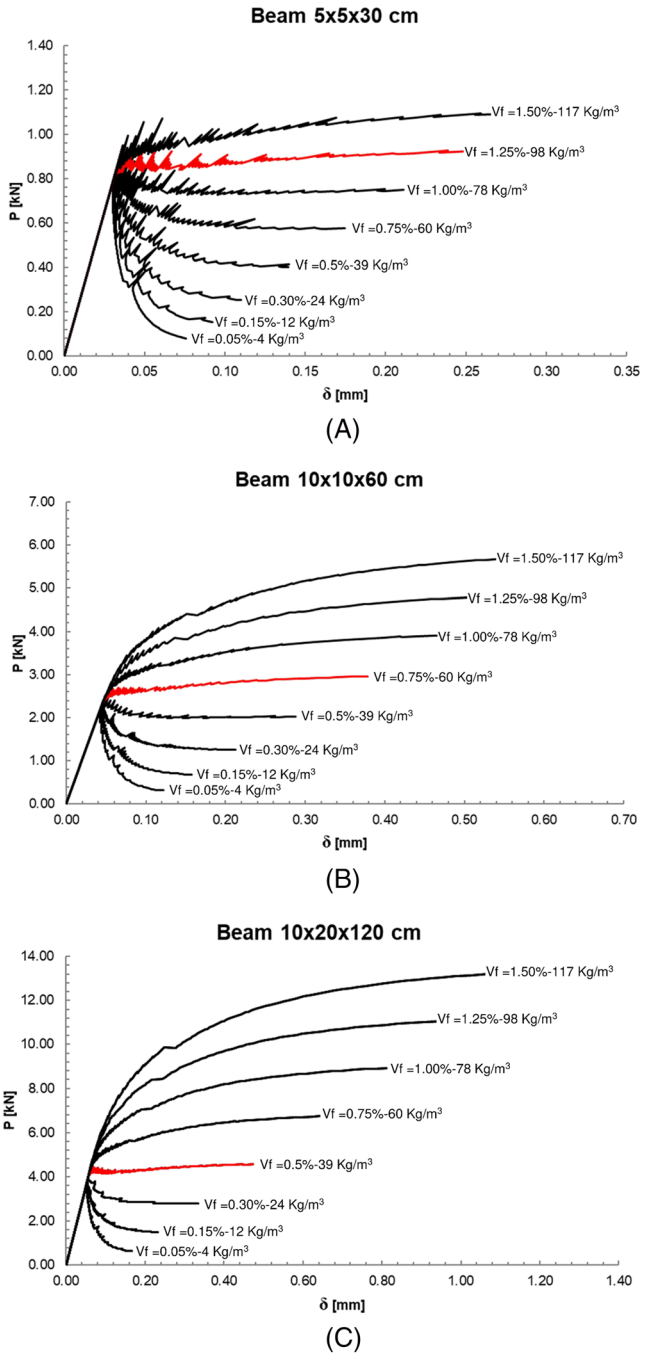

FIGURE 4 Design abacus based on fibre slippage mechanism. The numerical results are described in terms of load vs midspan deflection for beam size h = 50 mm (A); h = 100 mm (B); h = 200 mm (C). The red curve indicates the minimum reinforcement condition

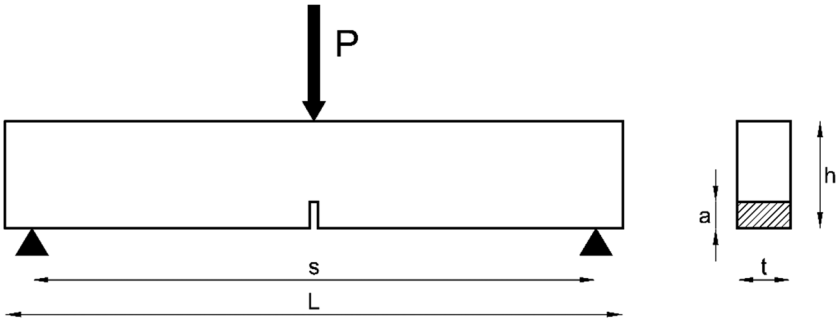

FIGURE 5 Three-point bending test geometry

In some cases, the postcracking response is characterized by local instabilities phenomena, represented by snap-back and snap-through due to the discontinuous location of the fibre reinforcements in the cracked cross section. As previously remarked, a ductile-to-brittle transition occurs in the global response. This transition is pointed out by the brittleness number, N_{PC}, as described in Equations (6) and (7), for yielding or slippage

FIGURE 6 Steel fibres adopted for three-point bending tests. From left to right: READYMESH MX-500, READYMESH MS-350, and READYMESH MM-150

TABLE 1 Steel fibre characteristics

Description	MM-150	MS-350	MX-500
Geometry			
Shape	Straight	Straight	Straight
Surface	Plane	Plane	Plane
Cross-section	Circular	Circular	Circular
End anchorage	None	Hooked ends	Double-hooked ends
Parameters			
l_f, mm	15	35	50
d_f, mm	0.75	0.75	0.75
λ_f	40	93	133
σ_u, MPa	1100	1100	1100

TABLE 2 FRC beams

ID	Height	Thickness	Length	Notch	MM-150	MS-350	MX-500	Tot.	
	h	t	L	a	V_f	V_f	V_f	V_f	
	[cm]	[cm]	[cm]	[cm]	[kg/m^3]	[kg/m^3]	[kg/m^3]	[%]	[kg/m^3]
FRC-5-04	5	5	30	1.5	2.1	4.2	-	0.08	6.2
FRC-5-15					5.2	10.4	-	0.20	15.6
FRC-5-75					25	49.9	-	0.96	75
FRC-5-100					33.3	66.6	-	1.28	100
FRC-10-04	10	10	60	3	2.1	-	4.2	0.08	6.2
FRC-10-15					5.2	-	10.4	0.20	15.6
FRC-10-75					25	-	49.9	0.96	75
FRC-10-100					33.3	-	66.6	1.28	100
FRC-20-04	20	10	115	5	2.1	-	4.2	0.08	6.2
FRC-20-15					5.2	-	10.4	0.20	15.6
FRC-20-75					25	-	49.9	0.96	75
FRC-20-100					33.3	-	66.6	1.28	100

bridging mechanism of the fibres. The transition is highlighted in each diagram, making possible the evaluation of the minimum amount of reinforcement in terms of fibre volume fraction, that is necessary for a globally stable response. Considering the same beam scale, under the assumption of yielding mechanism of the fibres, the amount of reinforcement required to have a stable structural response is about 5 times lower than that related to the fibre slippage mechanism, since $F_{P,yielding} = 5F_{P,slippage}$. On the other hand, Figures (3) and (4) show a decrease in the fibre volume fraction corresponding to the minimum reinforcement condition, when the structural size is increased. As predicted by Equations (6) and (7), the size effect is still described by the square root of the beam height h, regardless of the bridging mechanism considered.

3 | EXPERIMENTAL TESTS

TPB tests are carried out on FRC notched beams, as schematically represented in Figure 5. FRC beams were characterized by rectangular cross section, with a central precrack, in order to investigate the cracking behaviour of the midspan section.

The matrix of the composite material is made of a normal strength concrete C25/30, characterized by a compressive characteristic strength equal to 30 MPa. Three different types of steel fibres, supplied by AZICHEM Ltd, are adopted: straight steel fibre without end anchorages (READYMESH MM-150), straight fibre with single-hooked ends (READYMESH MS 350), and straight fibre with double-hooked ends (READYMESH MX-500), as pointed out in Figure 6. The steel fibres have diameter, d_f, equal to 0.75 mm; length, l_f, equal to 15, 35, and 50 mm; and aspect ratio, λ_f, varying from 40 to 133. All fibres have a tensile strength, σ_u, equal to 1100 MPa. Their mechanical and geometrical properties are summarized in Table 1.

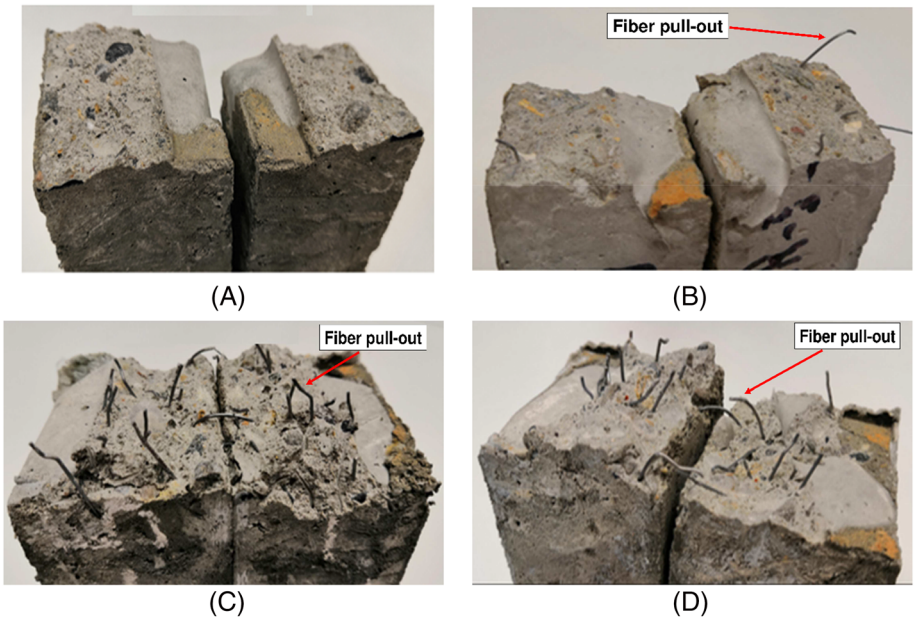

FIGURE 8 Fracture surfaces. A, FRC-5-04; B, FRC-5-15; C, FRC-5-75; D, FRC-5-100

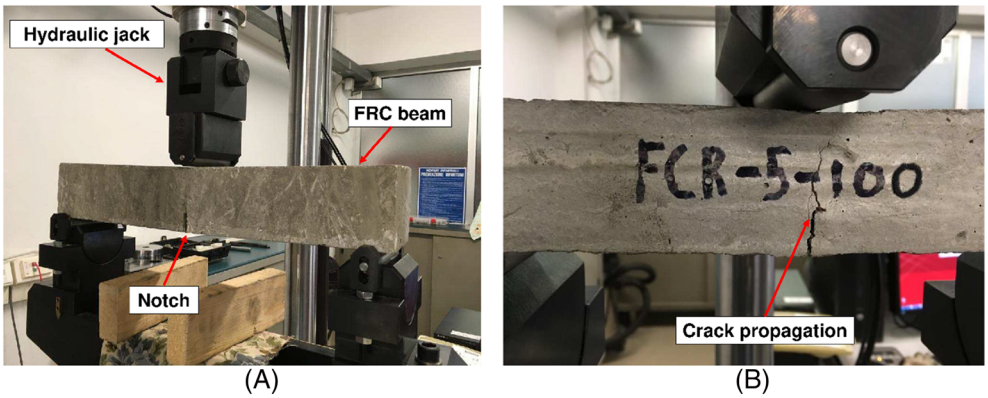

FIGURE 7 A, Experimental set-up; B, Crack propagation process

Concrete and fibres are combined in a dedicated mixer supplied by AZICHEM Ltd. and according to the above-mentioned fibre volume fractions. A uniform distribution of fibres in the matrix, without any signs of balling or clustering, is provided. The experimental campaign aims to investigate the effect of the dimensional scale and the fibre content on the mechanical response of FRC beams in bending; thus, three different beam sizes are tested, being the beam height, *h*, geometrically scaled by a factor equal to 1:2:4. For each specimen size, four different combinations of microfibre and macrofibre volume fractions, ranging from 0.08 to 1.28%, are considered (see Table 2).

Abbreviation: FRC: fibre-reinforced concrete.

The experimental setup is shown in Figure 7A. Experimental tests have been carried out under displacement control, by means of a hydraulic jack connected to an MTS testing machine with a maximum load capacity of 500 KN. A displacement rate of 4 μm/s is imposed, whereas the crack propagation process is carefully examined (Figure 7B).

Experimental tests provide the postcracking phase until the beam failure is obtained, in order to survey the fracture surface of each specimen at the end of each test (see Figures 8–10).

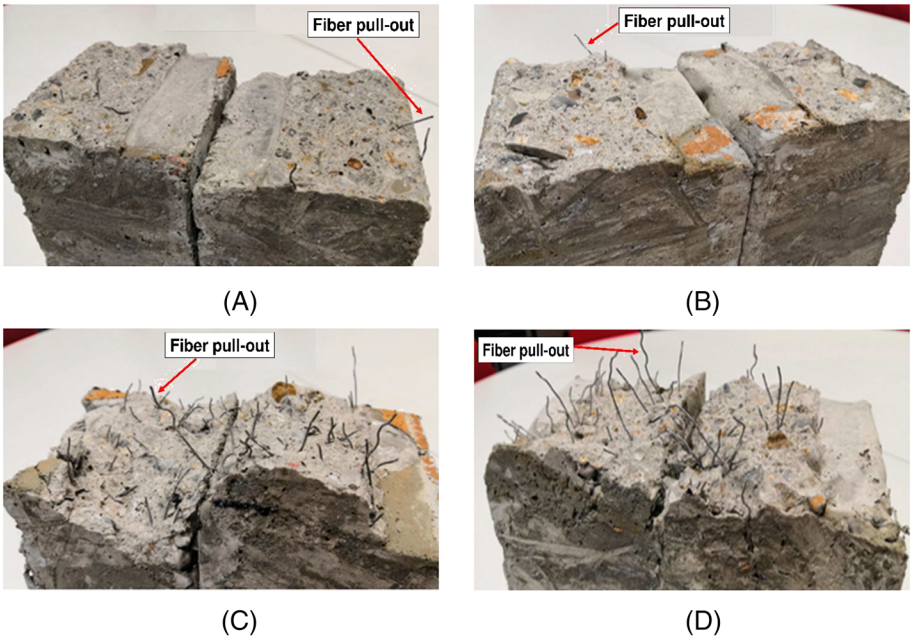

FIGURE 9 Fracture surfaces. A, FRC-10-04; B, FRC-10-15; C, FRC-10-75; D, FRC-10-100

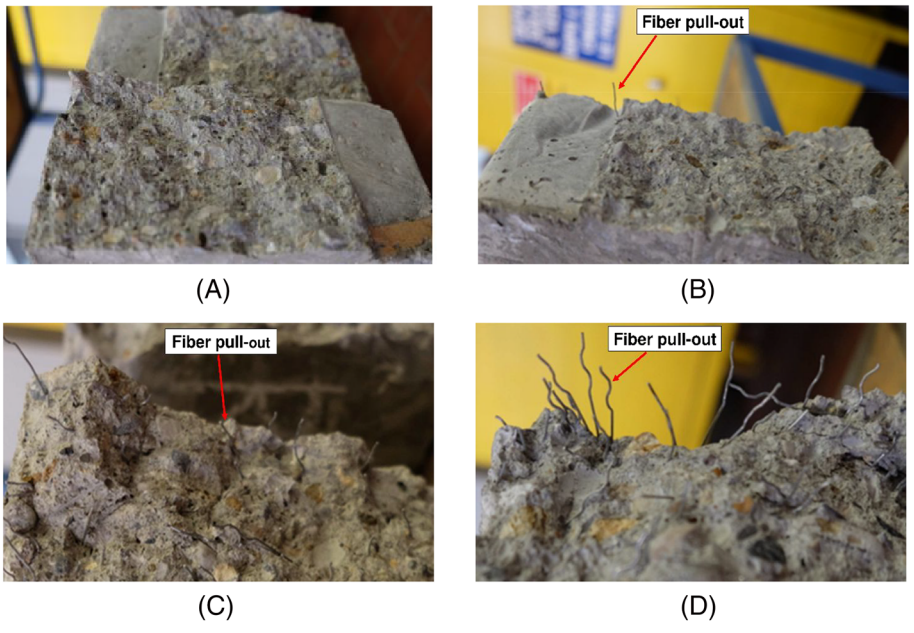

FIGURE 10 Fracture surfaces. A, FRC-20-04; B, FRC-20-15; C, FRC-20-75; D, FRC-20-100

4 | RESULTS AND DISCUSSION

In Figures 11–13, the flexural behaviour of the tested FRC beams is represented in terms of load vs midspan deflection, varying the beam size and the fibre content. For each specimen, numerical results obtained for both yielding (red curve) and slippage (blue curve) mechanism are compared with experimental results (black curve).

In all cases, experimental data fit with numerical results obtained in the slippage hypothesis, suggesting a pull-out mechanism between the matrix and the fibres, rather than steel fibre yielding. This response occurred also when macrofibres, MX-500 and MS-350, were used, even if the plastic flow of the steel fibres was expected in those cases, considering their hooked ends as able to provide mechanical anchorage. Instability phenomena during the crack propagation phase are experimentally verified. Considering the experimental curves, the postpeak response is characterized by a sawtooth-like shape. Snap-back instabilities are observed, identified by several vertical drops in the load vs midspan deflection diagrams. In addition, experimental tests confirm a ductile-to-brittle transition in the ultimate structural response of the FRC beams in flexure, as

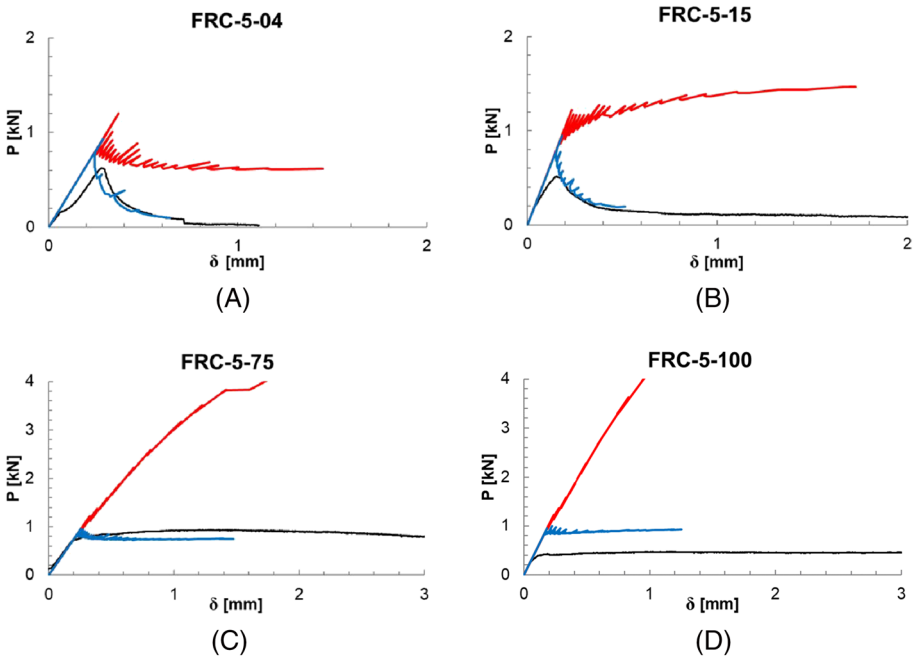

FIGURE 11 Experimental results vs numerical model for the specimen with h = 5 cm. A, FRC-5-04; B, FRC-5-15; C, FRC-5-75; D, FRC-5-100. The red and blue curves are obtained by the numerical model, in the case of yielding and slippage mechanism respectively. The black curve indicates the experimental results

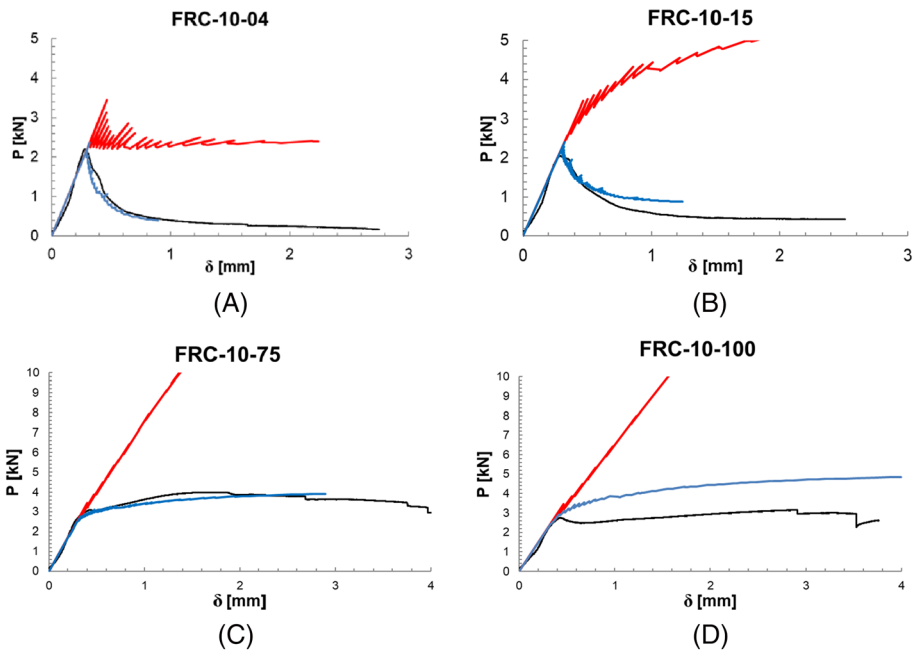

FIGURE 12 Experimental results vs numerical model for the specimen with h = 10 cm. A, FRC-10-04; B, FRC-10-15; C, FRC-10-75; D, FRC-10-100. The red and blue curves are obtained by the numerical model, in the case of yielding and slippage mechanism respectively. The black curve indicates the experimental results

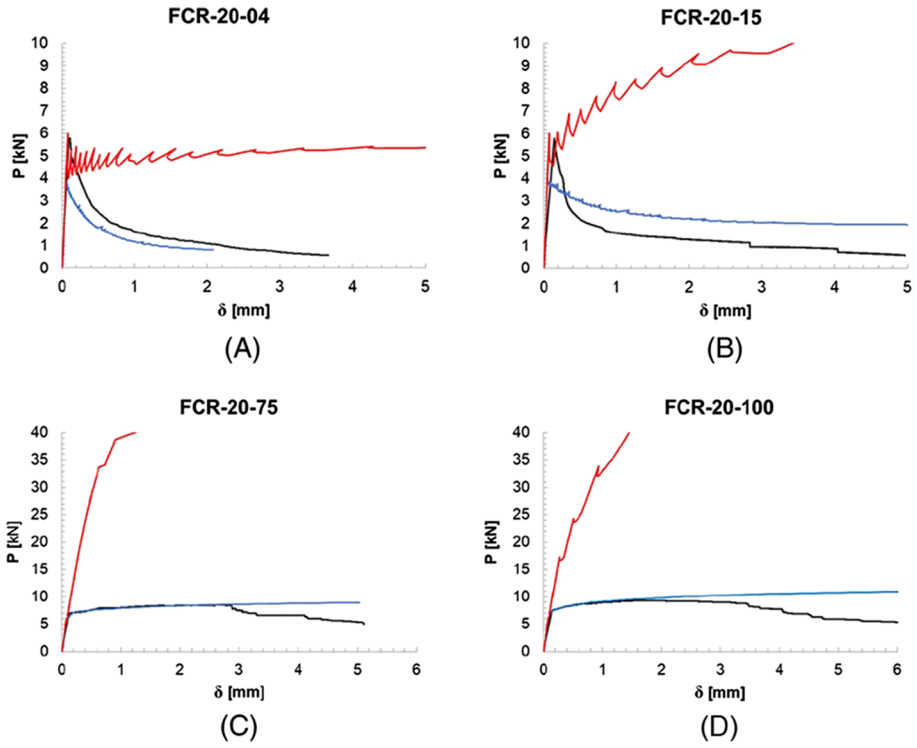

FIGURE 13 Experimental results vs numerical model for the specimen with h = 20 cm. A, FRC-20-04; B, FRC-20-15; C, FRC-20-75; D, FRC-20-100. The red and blue curves are obtained by the numerical model, in the case of yielding and slippage mechanism respectively. The black curve indicates the experimental results

predicted by the bridged crack model. For each beam scale, a different structural behaviour could be observed by varying the fibre volume fraction, V_f. Starting from a strain-softening structural response, occurring for low V_f values, the strain-hardening behaviours take place for large fibre volume fractions, V_f. This transition in the global response allows one to define the minimum reinforcement condition able to ensure a safe bearing capacity of FRC beams in flexure.

5 | CONCLUSIONS

In this work, an application of the bridged crack model has been proposed for predicting the postcracking behaviour of FRC members in bending. A numerical investigation is carried out in order to investigate the effect of the fibre volume content and the structural size on the mechanical response. With regard to the fibre bridging mechanism, the hypothesis of yielding law or slippage law of the fibres has been considered. In both cases, numerical results show that a ductile-to-brittle transition occurs in the mechanical response, governed by the brittleness number, N_P, in which the effects of the structural size and the fibre volume fraction are included. When the slippage mechanism controls the structural response, the brittleness number N_P takes into account also the aspect ratio of the fibre reinforcement. Experimental tests, carried out on notched FRC beams characterized by three different sizes and four fibre contents, show a good agreement between experimental and numerical results related to the slippage hypothesis, rather than the yielding one. The experimental results confirm also the transition in the global structural response by increasing the fibre volume ratio, V_f, revealing the effectiveness of the bridged crack model.

ACKNOWLEDGEMENTS

The authors gratefully acknowledge Luigi Aledda and AZICHEM Ltd. for their effective support.

ORCID

Federico Accornero https://orcid.org/0000-0002-9638-8411

REFERENCES

1. Naaman AE. High performance fiber reinforce cement composites. In: Chung DDL, ed. Vol. 1: High-Performance Construction Materials (Edited by Caijun Shi and Y L Mo) *Engineering Materials for Technological Needs*. Singapore: World Scientific Publishing Co. Pte. Ltd; 2008:91-153.
2. Carpinteri, A. (1981) A fracture mechanics model for reinforced concrete collapse. Proceedings of the IABSE Colloquium on Advanced Mechanics of Reinforced Concrete, Delft, 17–30.
3. Carpinteri A. Stability of fracturing process in RC beams. J Struct Eng (ASCE). 1984;110(3):544-558.

4. Carpinteri A, Carpinteri A. Hysteretic behavior of RC beams. J Struct Eng (ASCE). 1984;110(9):2073-2084.
5. Carpinteri A, Massabò R. Continuous vs discontinuous bridged crack model of fiber-reinforced materials in flexure. Int J Solids Struct. 1997;34:2312-2338.
6. Carpinteri A, Massabò R. Reversal in failure scaling transition of fibrous composites. J Eng Mech (ASCE). 1997;123(2):107-114.
7. Bosco C, Carpinteri A. Discontinuos constitutive response of brittle matrix fibrous composites. J Mech Phys Solids. 1995;43(2):261-274.
8. Carpinteri A, Puzzi S. The bridged crack model for the analysis of brittle matrix fibrous composites under repeated bending loading. J Appl Mech. 2007;74(6):1239-1246.
9. Carpinteri A, Accornero F. The bridged crack model with multiple fibers: local instabilities, scale effects, plastic shake-down, and hysteresis. Theor Appl Fract Mech. 2019;104:102351
10. Carpinteri A, Accornero F. Residual crack opening in fiber-reinforced structural elements subjected to cyclic loading. Strength Fract Complex. 2019;1:1-12.
11. Taylor M, Lydon FD, Barr BIG. Toughness measurements on steel fiber-reinforced high strength concrete. Cement Concr Compos. 1997;19(4):329-340.
12. Lee MK, Barr BIG. A four-exponential model to describe the behaviour of fibre reinforced concrete. Mater Struct. 2004;37(7):464-471.
13. Barros JOA, Cunha VMCF, Ribeiro AF, Antunes JAB. Post-cracking behaviour of steel fibre reinforced concrete. Mater Struct. 2005;38(1):47-56.
14. Holschemacher K, Müeller T, Ribakov Y. Effect of steel fibres on mechanical properties of high-strength concrete. Mater Des. 2010;31(5):2604-2615.
15. Fantilli AP, Chiaia P, Gorino A. Fiber volume fraction and ductility index of concrete beams. Cement Concr Compos. 2016;65:139-149.
16. Bosco C, Carpinteri A, Debernardi PG. Minimum reinforcement in high-strength concrete. J Struct Eng (ASCE). 1990;116(2):427-437.
17. Bosco C, Carpinteri A, Debernardi PG. Fracture of reinforced concrete: scale effects and snap-back instability. Eng Fract Mech. 1990;35(4-5):665-677.
18. Lacidogna G, Accornero F. Elastic, plastic, fracture analysis of masonry arches: a multi-span bridge case study. Curved Layered Struct. 2018;5(1):1-9.
19. Accornero F, Lacidogna G, Carpinteri A. Medieval arch bridges in the Lanzo valleys, Italy: case studies on incremental structural analysis and fracturing benefit. J Bridge Eng (ASCE). 2018;23(7):05018005
20. Carpinteri A, Accornero F. Multiple snap-back instabilities in progressive microcracking coalescence. Eng Fract Mech. 2018;187:272-281.
21. Lacidogna G, Accornero F, Carpinteri A. Influence of snap-back instabilities on Acoustic Emission damage monitoring. Eng Fract Mech. 2019;210:3-12.

How to cite this article: Accornero F, Rubino A, Carpinteri A. Ductile-to-brittle transition in fibre-reinforced concrete beams: Scale and fibre volume fraction effects. *Mat Design Process Comm*. 2020;1–11. https://doi.org/10.1002/mdp2.127